EUROPEAN ORGANIZATION FOR NUCLEAR RESEARCH

# MEASUREMENT OF DIRECT CP VIOLATION WITH THE EXPERIMENT NA48 AT CERN

Sandro Palestini [a)]
CERN, 1211 Geneva 23, Switzerland [b)]

## Abstract

Direct CP violation is studied in two pion decays of the neutral kaon. Using data collected in the first beam period in 1997, the result for the parameter $\mathrm{Re}\,(\varepsilon'/\varepsilon)$ is $(18.5 \pm 4.5(\mathrm{stat}) \pm 5.8(\mathrm{syst})) \times 10^{-4}$.

*Talk presented at the EPS–HEP 99 Conference*
*Tampere, Finland, July 15–21, 1999*

[a)] On behalf of the NA48 Collaboration: Cagliari, Cambridge, CERN, Dubna, Edinburgh, Ferrara, Firenze, Mainz, Orsay, Perugia, Pisa, Saclay, Siegen, Torino, Vienna, Warsaw.
[b)] Permanent address: INFN, sez. Torino, 10125 Torino, Italy.

## 1 Introduction

Two pion decays of $K_L$ [1] established the violation of the symmetry CP. The main effect is due to a small component of CP $= +1$ eigenstate in $K_L$, which decays into two pions in a way similar to $K_S$. Direct CP violation is found in the deviation from unity of the double ratio of decay rates:

$$\begin{aligned} R &= \frac{\Gamma(K_L \to \pi^0\,\pi^0\,)/\,\Gamma(K_S \to \pi^0\,\pi^0\,)}{\Gamma(K_L \to \pi^+\pi^-)/\,\Gamma(K_S \to \pi^+\pi^-)} \\ &\simeq 1 - 6 \times \mathrm{Re}\,(\varepsilon'/\varepsilon)\,. \end{aligned}$$

First evidence for non–vanishing $\mathrm{Re}\,(\varepsilon'/\varepsilon)$ [2] was not supported by a different experiment [3], while a recent result [4] confirms the effect.

The Standard Model provides a natural mechanism for direct CP violation, but current predictions [5, 6] are affected by significant computational uncertainties.

The experiment NA48 has been designed for an accurate measurement of $\mathrm{Re}\,(\varepsilon'/\varepsilon)$, using an approach with significant improvements over the techniques used previously [2, 3]. The first results, from data collected in 1997, are presented here.

## 2 Experimental technique

In order to minimize the sensitivity to detector efficiency, to variations in beam intensity, and to accidental activity, the experiment [7] is designed to collect data simultaneously in the four channels $K_L$, $K_S \to \pi^0\,\pi^0$, $\pi^+\pi^-$, with the kaon energy in the interval 70–170 GeV. Two neutral beams are used: the $K_L$ beam is produced 126 m (corresponding on average to 21 $K_S$ lifetimes $\tau_S$) upstream of the nominal decay region. The $K_S$ beam is produced 6 m (one $\tau_S$) upstream of the decays region. The two beams, which are 68 mm apart as they pass the final collimator, converge and cross at the position of the electromagnetic (e.m.) calorimeter, 115 m downstream. Figure 1 shows the layout of the decay region and the main detector components. In order to minimize the difference in acceptance between $K_L$ and $K_S$, only decays occurring in the upstream part are used, requiring $0 < \tau < 3.5\,\tau_S$, which corresponds to $0 < z < 21$ m on average.

The identification $K_L$ vs. $K_S$ is done looking for a time coincidence between a kaon decay measured in the main detector, and the detection of a proton in the beam directed

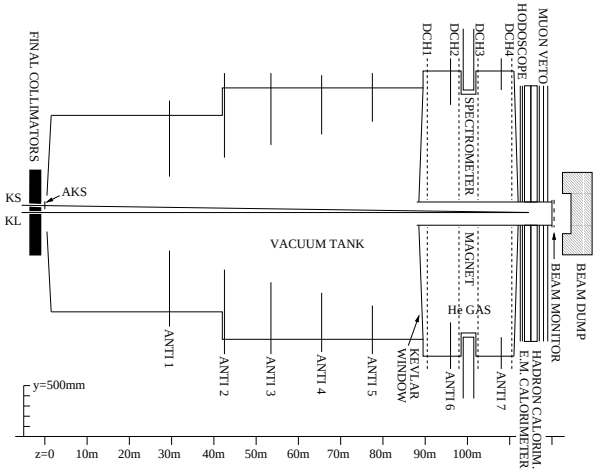


Figure 1: Layout of the main detector components.

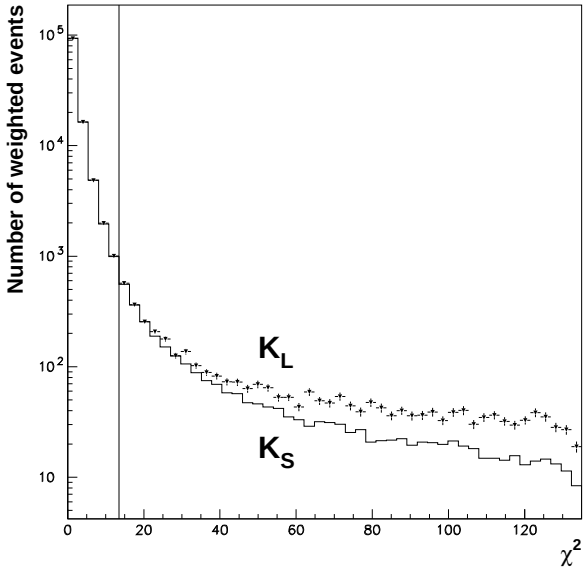


Figure 2: Distribution of $\chi^2$ for $K_L$ and $K_S \to \pi^0\,\pi^0$, normalized in the first bin. The excess of $K_L$ candidates in the region $\chi^2 > 36$ is used to compute the background due to $3\pi^0$ in the signal region ($\chi^2 < 13.5$).

to the $K_S$ production target. This is done by means of a finely segmented scintillation counter (tagger).

## 3 Event selection

Decays to $\pi^0\,\pi^0$ are triggered in a 40 MHz pipeline, which computes the number of clusters, the total energy and the first and second momenta of the energy distribution in the calorimeter. This allows to select $K^0$ candidates with decay time $\tau < 5\,\tau_S$. The trigger inefficiency is equal to $(12 \pm 4) \times 10^{-4}$. Off–line, the four clusters are paired to check that their invariant mass is compatible with the $\pi^0$ mass (resolution 1.1 MeV/$c^2$). The corresponding $\chi^2$ distribution is shown in figure 2, where the difference between $K_L$ and $K_S$ is due to background from $3\pi^0$ events, and is equal to $(8 \pm 2) \times 10^{-4}$.

In $\pi^+\pi^-$ decays, a first level trigger is based on the scintillation hodoscope and the total energy measured by the calorimeters. This is down–scaled by two, and prompts the second level trigger, which uses drift chamber data to reconstruct vertices and compute invariant masses and decay times. The trigger efficiency is computed on samples of events from auxiliary, down–scaled triggers, and found equal to $(91.0 \pm 0.1)$ %. The off–line selection includes tighter cuts on invariant mass (2.5 MeV/$c^2$ resolution) and transverse momentum. The background from semileptonic $K_L$ decays is further rejected using the muon hodoscope, and the $E/P$ ratio from the e.m. calorimeter and the spectrometer. The total background in the charged mode is $(23 \pm 4) \times 10^{-4}$ (see figure 3).

Figure 4 shows the distribution of the time difference between the tagger (on the $K_S$ proton beam line) and the main detector, where the event time is measured by the e.m. calorimeter, and by the scintillation hodoscope, respectively for neutral and charged decays. The coincidence window is $\pm 2$ ns. For $\pi^+\pi^-$, the rate of inefficiency (resulting in a $K_S$ being misidentified as a $K_L$) and of accidental coincidences (tagging a $K_L$ as $K_S$) are measured applying a selection on the vertex position (figure 4b). In the neutral mode, accidental tagging is measured in off–set time intervals, and the efficiency is obtained comparing the response of the calorimeter and the scintillation hodoscope in

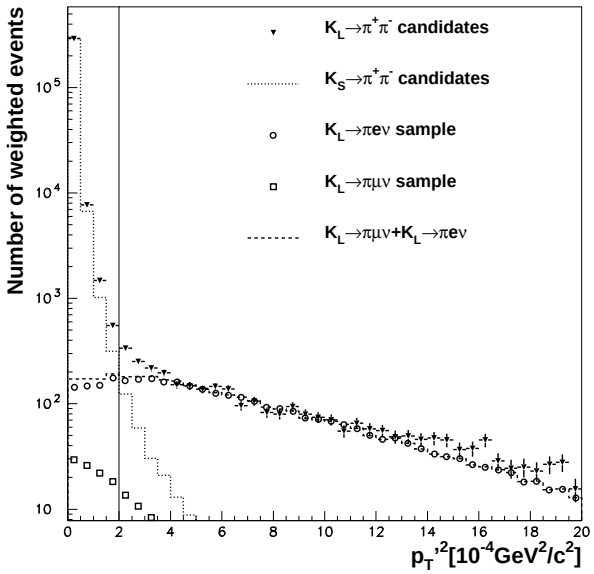


Figure 3: Distribution of $p_t'^2$ for $K_L$ candidates, $K_S$ events (normalized in the first bin), and background from $K_{e3}$ and $K_{\mu 3}$ decays. The signal region is $p_t'^2 < 2\times 10^{-4}$ GeV$^2/c^2$.

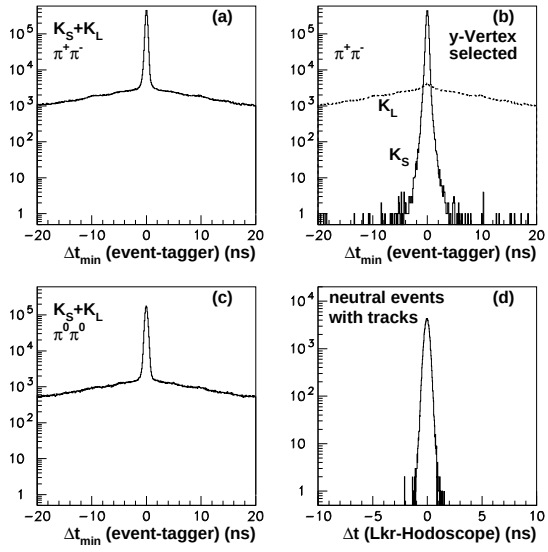


Figure 4: (a) Distribution of the minimum difference between tagger and event times for $\pi^+\pi^-$ decays. The peak corresponds to $K_S$ events. (b) The same, separated into $K_S$ and $K_L$ events using the vertex position. (c) as (a) for $\pi^0\,\pi^0$ mode. (d) Coincidence time for neutral events with tracks.

Table 1: Statistical samples, in thousands of events.

| $K_L \to \pi^0\,\pi^0$ | $K_S \to \pi^0\,\pi^0$ | $K_L \to \pi^+\pi^-$ | $K_S \to \pi^+\pi^-$ |
|---|---|---|---|
| 489 | 975 | 1,071 | 2,087 |

events with photon conversion or Dalitz decays (figure 4d). The double ratio $R$ is affected by the differences of the tagging errors between neutral and charged modes. The tagging inefficiency is about $1 \times 10^{-4}$, with a difference of $(0 \pm 1) \times 10^{-4}$ between the two modes. The rate of accidental tagging is 11.2 % on average, and is measured to be $(10 \pm 5) \times 10^{-4}$ larger in the neutral mode.

Table 1 shows the number of events in each channel, after background and tagging corrections.

## 4 Systematic corrections and uncertainties

The difference between the decay distributions of $K_L$ and $K_S$ in the 3.5 $\tau_S$ accepted interval implies a difference in acceptance, which requires a correction to the measured value of $R$. This effect is reduced by weighting the $K_L$ events used in the double ratio with a function of the proper decay time $\tau$, proportional to the expected ratio of $K_S$ and $K_L$ decay rates. In the charged mode, residual differences in acceptance due to the beam geometries are minimized by a kinematical cut which rejects asymmetric decays. Finally, to be independent of the $\pm 10$ % difference in the energy spectra of the two beams, the analysis is performed in 5 GeV wide energy bins. The result of this procedure is an acceptance correction of $(29 \pm 12) \times 10^{-4}$, where most of the uncertainty is due to Monte Carlo statistics.

The effects of accidental activity are minimized by taking data simultaneously in the four channels. The rate of accidentals is measured to be equal for $K_L$ and $K_L$ events within the error of 1 %. A small correction to $R$ is computed using a sample of events overlayed

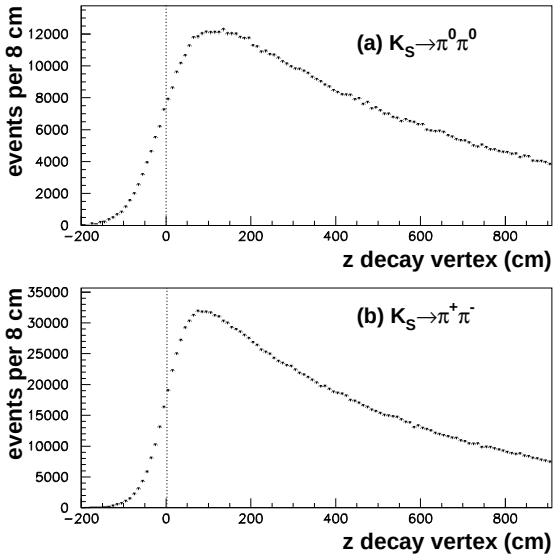


Figure 5: Distribution of the reconstructed decay vertex in $K_S$ events for (a) the $\pi^0\,\pi^0$ mode and (b) the $\pi^+\pi^-$ mode. The rising edge corresponds to the position of the veto–counter (dotted line).

Table 2: Corrections and uncertainties to $R$, in $10^{-4}$ units.

| | | | | |
|---|---|---|---|---|
| Tagging errors | + | 18 | ± | 11 |
| $\pi^+\pi^-$ trigger efficiency | + | 9 | ± | 23 |
| Acceptance | + | 29 | ± | 12 |
| Accidental effects | − | 2 | ± | 14 |
| $\pi^0\,\pi^0$ background | − | 8 | ± | 2 |
| $\pi^+\pi^-$ background | + | 23 | ± | 4 |
| Beam scattering | − | 12 | ± | 3 |
| Energy scale and linearity | | | ± | 12 |
| Charged vertex | | | ± | 5 |
| Total correction | + | 57 | ± | 35 |

with data selected by random triggers, hence obtaining a sample with artificially higher accidental activity. Another small correction is due to beam scattering in the collimators of the $K_L$ beam.

Particular care is taken in the definition of the accepted decay range. For $K_S$ decays, the upstream end of the fiducial volume is defined by a veto–counter placed across the beam. The absolute energy scale of the e.m. calorimeter is tuned by checking the distribution of the reconstructed events against the position of the veto–counter (figure 5). For $K_L$ decays, the definition of the boundaries $0 < \tau < 3.5\,\tau_S$ relies on an accurate knowledge of the energy scale, and of the linearity of the calorimeter response. Linearity and uniformity are studied with electrons from $K_{e3}$ events continuously recorded, and with auxiliary data. The task is facilitated by the intrinsic high stability of the detector (the absolute energy scale was stable within $\pm\,5 \times 10^{-4}$ throughout the entire run). The total contribution to the systematic error in $R$ is $\pm\,12 \times 10^{-4}$. In the charged mode, the fit to the $K_S$ veto–counter provides a check on length scales and alignment, quantified in a small systematic uncertainty.

Table 2 lists all the corrections applied to the double ratio. The uncertainties in the first four lines are dominated by the statistics of the control sample used in each study.

## 5 Result

Figure 6 shows the result for $R$ in the different energy bins. Corrections for trigger efficiency, tagging, background and acceptance are included in each bin. The overall average is $R = 0.9889 \pm 0.0027 \pm 0.0035$, where the first error is from the statistical fluctuation in the event samples, and the second is from the uncertainties in table 2. The three blank points at the extremes were studied as an additional check on systematic effects, and including them would not modify significantly the average value. The corresponding result for the parameter describing direct CP violation is:

$$\mathrm{Re}\,(\varepsilon'/\varepsilon) = (18.5 \pm 4.5 \pm 5.8) \times 10^{-4}$$

or, combining the errors in quadrature, $\mathrm{Re}\,(\varepsilon'/\varepsilon) = (18.5 \pm 7.3) \times 10^{-4}$.

In figure 7 this new result is compared with some predictions based on the Standard Model [6] and other measurements [2, 3, 4]. The existence of direct CP violation in the neutral kaons is confirmed at the level of $\mathrm{Re}\,(\varepsilon'/\varepsilon) \simeq 20 \times 10^{-4}$.

A more accurate knowledge of $\mathrm{Re}\,(\varepsilon'/\varepsilon)$ will be possible with data collected by NA48 in 1998, 1999, and 2000. An increase of the statistical samples by a factor $\simeq$ 10 is expected,

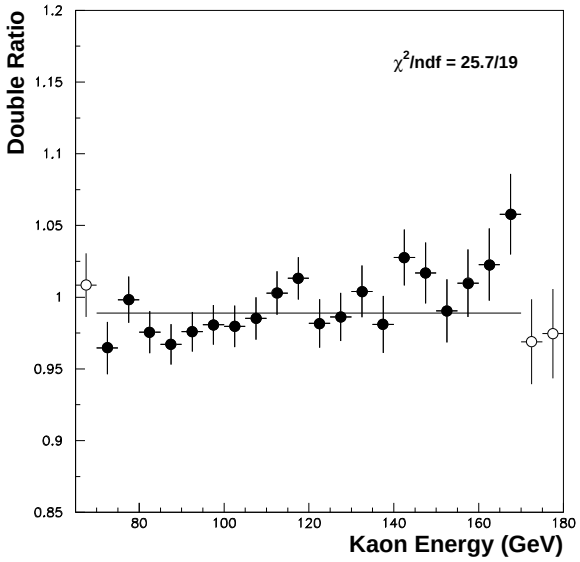


Figure 6: Measured double ratio in energy bins. The points used for the measurement of $\mathrm{Re}\,(\varepsilon'/\varepsilon)$ are shown in black.

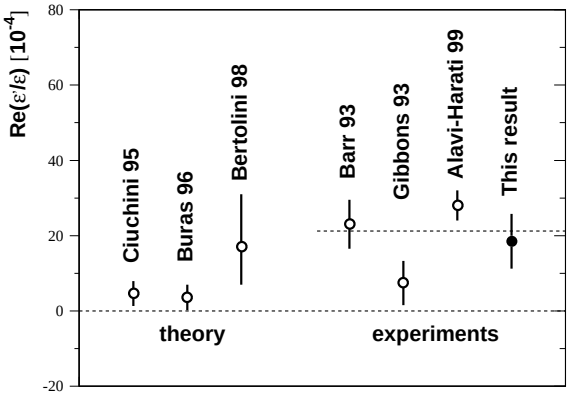


Figure 7: Comparison of prediction and experimental results.

together with a significant reduction in the systematic uncertainties.

## References


[1] J.H. Christenson et al. 1964 *Phys. Rev. Lett.* **13** 138.

[2] H. Burkhardt et al. 1988 *Phys. Lett.* B **206** 169; G. Barr et al. 1993 *Phys. Lett.* B **317** 233.

[3] L.K. Gibbons et al. 1993 *Phys. Rev. Lett.* **70** 1203.

[4] H. Nguyen, these proceedings; A. Alavi-Harati et al. 1999 *Phys. Rev. Lett.* **83** 22.

[5] For a review, see G. Buchalla, these proceedings.

[6] M. Ciuchini et al. 1995 *Z. Phys.* C **68** 239;
A. Buras et al. 1996 *Phys. Lett.* B **389** 749;
S. Bertolini et al. 1998 *Nucl. Phys.* B**514** 93.
See also T. Hambye et al. 1998 *Phys. Rev.* D **58** 14017; and A. Soni, these proceedings.

[7] For more details on the detector and the analysis see V. Fanti et al. 1999 to appear on *Phys. Lett.* B (preprint CERN–EP/99–114, hep–ex/9909022).